Environmental Pollution 384 (2025) 127002

Contents lists available at ScienceDirect

Environmental Pollution

journal homepage: www.elsevier.com/locate/envpol

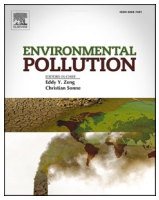

Epigenetic and genotoxic effects of tritium in marine mussels: Comparing waterborne and metal-associated forms☆

Maria Florencia Ferreira [a], Andrew Turner [b], Mickaël Payet [c], Olivier Debellemaniere [c], Christian Grisolia [c], Veronique Malard [d], Michael N. Moore [a,e,f], Awadhesh N. Jha [a,*]

[a] School of Biological and Marine Sciences, University of Plymouth, Plymouth, PL4 8AA, United Kingdom
[b] School of Geography, Earth and Environmental Sciences, University of Plymouth, Plymouth, PL4 8AA, United Kingdom
[c] CEA, IRFM, Saint Paul Lez Durance, F-13108, France
[d] Aix Marseille Univ, CEA, CNRS, BIAM, Saint Paul-Lez-Durance, France
[e] European Centre for Environment & Human Health (ECEHH), University of Exeter Medical School, Peter Lanyon Building 12, Penryn, Cornwall, TR10 8RD, United Kingdom
[f] Plymouth Marine Laboratory, Prospect Place, The Hoe, Plymouth, PL1 3HD, United Kingdom

ARTICLE INFO

Keywords:
DNA damage
DNA methylation
Ionising radiation
Marine mussels
Tritiated steel particles
Tritiated water

ABSTRACT

Tritium (^{3}H), an isotope of hydrogen, is a by-product of the nuclear industry. Decommissioning and normal operations of nuclear facilities can generate tritiated stainless-steel particles (T-SSPs) that could be unintentionally released into the environment. Considering tritium's physicochemical properties and the proximity of nuclear facilities to water bodies, assessing the behaviour and potential effects of these particles in the aquatic environment is imperative. In the present study, marine mussels, *Mytilus galloprovincialis,* were exposed to: (a) hydrogenated, non-radioactive stainless-steel particles (H-SSPs) (10 mg L^{-1}) (b) T-SSPs (1 and 10 MBq L^{-1}) and (c) tritiated water (HTO) (0.50 and 5.0 MBq L^{-1}) for 5 h and 7 d. Exposure to T-SSPs resulted in significant DNA damage in mussel haemocytes. Tritium bioaccumulation was significantly higher in the digestive gland (DG), regardless of the exposure duration to T-SSPs. Positive correlation between tritium in DG tissues and DNA indicates that tritium is internalised in the cell. After 7 d, global DNA methylation increased in gills exposed to both 1 MBq L^{-1} of T-SSPs and 5 MBq L^{-1} of HTO treatments. In the DG tissue, DNA methylation increased following exposure to tritium (water and particulate forms) compared to H-SSPs, suggesting a tissue-specific and pollutant-dependent response. Our findings highlight the enhanced bioaccumulation of T-SSPs compared to HTO. Multivariate analyses of the results suggested an overall stress response in mussels exposed to T-SSPs compared to HTO exposure and controls. Potential epigenetic effects will require more attention as they can bring knowledge across levels of biological organisation and about the transgenerational impact of radionuclides.

1. Introduction

Tritium (^{3}H), a radioisotope of hydrogen, is present during fission and fusion nuclear energy production systems (Grisolia et al., 2019; Nie et al., 2021). About 99 % of tritium is discharged by nuclear facilities as tritiated water (HTO), while HTO present in the atmosphere also reaches the ocean (Oms et al., 2019). In the environment and in biological systems, tritium is also involved in indistinguishable chemical reactions like hydrogen and associates with biomolecules (e.g., carbohydrates, proteins, DNA). Organically bound tritium (OBT) has the potential to bioaccumulate in tissues, persist in tissues longer compared to HTO and biomagnify in the food chain (Jaeschke et al., 2011; Jaeschke and Bradshaw, 2013; Eyrolle et al., 2018). In nuclear facilities, some tritium also has the potential to be associated and discharged with steel and

Abbreviations: **ADME**, absorption, distribution, metabolism and excretion; **AM**, adductor muscle; **DG**, digestive gland; **DSBs**, DNA double strand breaks; **FPG**, formamidopyrimidine DNA glycosylase; **H-SSPs**, hydrogenated (non-radioactive) stainless-steel particles; **HTO**, tritiated water; **MVA**, multivariate analysis; **NTA**, nanoparticle tracking analysis; **OBT**, organically bound tritium; **OD**, optical density; **PCA**, principal component analysis; **ROS**, reactive oxygen species; **SCGE**, single cell gel electrophoresis; **SW**, seawater; **T-SSPs**, tritiated stainless-steel particles.

☆ This paper has been recommended for acceptance by Mingliang Fang.

* Corresponding author.
E-mail address: a.jha@plymouth.ac.uk (A.N. Jha).

https://doi.org/10.1016/j.envpol.2025.127002
Received 14 May 2025; Received in revised form 7 August 2025; Accepted 15 August 2025
Available online 16 August 2025

cement particles resulting from normal operations as well as during facility dismantling (Ferreira et al., 2023; Lamartiniere et al., 2022; Liger et al., 2018).

Studies have shown β-particles emitted from ^{3}H to be efficient in producing DNA strand breaks, the repair of which is critical for cell survival (Adam-guillermin et al., 2012; Ferreira et al., 2023; Jha, 2008; Jha et al., 2005; Koturbash et al., 2006; Reisz et al., 2014). Interestingly, in vitro studies have suggested that when tritiated stainless-steel particles (T-SSPs) are deposited for 24 h on the surfaces of cells, a greater DNA damaging effect is produced compared to HTO (Mentana et al., 2022). Ionising radiation can also influence a tissue specific DNA methylation pattern in mice and other aquatic species (Belli and Tabocchini, 2020; Kong et al., 2016; Kovalchuk et al., 2004; Pogribny et al., 2004; Trijau et al., 2018), but limited information is available for marine invertebrates (Horemans et al., 2019). Genome-wide hypomethylation is often viewed as a sign of genome destabilisation, leading to increased mutation rates (Jaenisch and Bird, 2003; Kovalchuk and Baulch, 2008; Wei et al., 2019), while the regulation of gene transcription by DNA methylation varies among taxa (Gavery and Roberts, 2010; Horemans et al., 2019; Wang et al., 2006).

Marine bivalves of the genus *Mytilus*, such as *M. galloprovincialis*, represent ideal sentinel species in biomonitoring programmes such as 'mussel watch' (Barreira et al., 2024). As filter feeding organisms, they tend to accumulate different pollutants, including tritium, in their tissues (Jong et al., 2022; Wang et al., 2021a; Ward et al., 2019; Jha et al., 2005; Jaeschke et al., 2011).

Our previous study has shown that *M. galloprovincialis* can bioaccumulate hydrogenated (non-radioactive analogue) stainless-steel particles (H-SSPs) after acute and sub-chronic exposures, although no DNA damage was found in mussel haemocytes (Vernon et al., 2022). In order to further understand the potential biological consequences of radioactive stainless-steel particles, the present study aimed to (a) characterise the behaviour of T-SSPs in seawater, (b) determine tissue-specific bioaccumulation of T-SSPs in *M. galloprovincialis*, (c) assess the potential genotoxic and epigenetic effects of these particles, and (d) integrate biological or biomarker responses and bioaccumulation data through multivariate analysis. Overall, the study hypothesised that, compared to HTO and H-SSPs, exposure to T-SSPs would result in higher bioaccumulation and more pronounced genotoxic and epigenetic effects in marine mussels.

2. Materials and methods

2.1. Particle behaviour in seawater

H-SSPs were prepared and used concurrently as a non-radioactive control for the experiments while using T-SSPs as described by Slomberg et al. (2024). A stock solution of H-SSPs (1 mg mL^{-1}) was prepared with 10 mg of H-SSPs in 10 mL deionised water in Falcon tubes (50 mL). Non-filtered and 1 mL filtered water samples (0.22 μm) were processed in duplicate using a nanoparticle tracking analysis (NTA, Nanosight®, LM10, Version 2.2; Malvern Panalytical, UK) to study the concentration and hydrodynamic diameters of H-SSPs particles in suspension. Samples were collected to determine particle behaviour and dissolution in seawater before performing the experiments with T-SSPs. Filtered seawater samples were collected to determine potential release of tritium as tritiated water and to determine small particle (<0.22 μm) release.

2.2. Exposures of mussels to H-SSPs, T-SSPs and HTO

Mytilus galloprovincialis (shell length ~ 45 mm) were collected from a pristine site in Cornwall (UK) and maintained in accordance with earlier studies carried out in our laboratory (Dallas et al., 2013; Pearson et al., 2018; Ferreira et al., 2024). Briefly, mussels were maintained in UV-treated, filtered (<10 μm), aerated, natural seawater (SW) (salinity = 31.8, pH = 7.9) under a 12:12 h photoperiod at 15 °C and were fed a solution of *Isochrysis galbana* algae (1×10^5 cells mL^{-1}, Reed Mariculture, Campbell, CA, USA) every other day. Twenty, 2-L beakers containing 1.5 L of filtered seawater at 20 °C and three mussels in each beaker were used for the exposures (i.e., two beakers and six mussels per treatment) and two different exposure scenarios, 5 h and 7 d.

The tritium activity concentration was selected based on projections of the dose to be received by mussels, with the concentration 1000 μg L^{-1} equal to an activity level of 1 MBq L^{-1}. As noted in previous literature, our selected tritium levels, 1 and 10 MBq L^{-1}, result in dose rates ranging from 3.13 to 7.90 μGy h^{-1} and 15.13–18.49 μGy h^{-1}, respectively, for the selected exposure periods (Dallas et al., 2016b). This dose range represents below and above the generic (all species) screening value of 10 μGy h^{-1} (Dallas et al., 2016b). The exposure periods used in the present study were selected based on previous findings with non-tritiated steel particles (i.e. H-SSPs), where the methodology was also validated (Vernon et al., 2022). These periods also reflect realistic scenarios of short-term effluent releases or accidental exposures (Hanslík et al., 2017; Kaizer et al., 2024; Varlam et al., 2005). Each beaker was covered and aeration was set up using a glass Pasteur pipette connected to the aeration system. Evaporation rate was determined previously in beakers containing SW only and <10 % was determined after 7 d (data not shown).

Beakers were dosed once with 1 or 10 MBq L^{-1} of T-SSPs. In addition, a SW control, an H-SSPs control (10 mg L^{-1}) and HTO (0.50, 5.0 MBq L^{-1}) were run in parallel to account for waterborne tritium release (~50 %) in SW from T-SSPs according to previous experiments (Jha et al., 2022). During the exposure period, no water change was conducted. Mussels were not fed during the exposure period, and there was no mortality or spawning during the experiment. Filtered (<0.22 μm) and non-filtered SW samples (1 mL) were collected every alternate day, with filtered SW determining potential release of tritium as HTO and to determine small particles (<0.22 μm) release as described in section 2.1. Liquid scintillation cocktail (4 mL) (Ecosint, Scientific Laboratory Supplies, UK) was added to each sample, and read using a PerkinElmer Tricarb liquid scintillation counter, with a chemiluminescence quench correction curve. There was no indication of a drop in tritium concentration (activity) over the two exposure periods. (i.e., 5 h and 7 d).

At the end of both exposure periods, haemolymph samples were collected from the adductor muscle (AM) to assess DNA damage in the haemocytes using single cell gel electrophoresis (SCGE) or the comet assay as described previously (Dallas et al. 2016 a; b; Ferreira et al., 2023). Following collection of haemolymph samples, mussels were dissected and individual tissues (AM, DG, gill, foot, mantle and other soft tissues) were collected to assess bioaccumulation of the particles and perform other biological assays. In addition, subsamples of dissected tissues (i.e., 20 mg of gills and DG) from each mussel were blotted and placed in individual Eppendorf tubes and stored at −80 °C until further DNA extraction and determination of methylation patterns. These subsamples were only collected from mussels exposed for 7 d due to logistic limitations.

2.3. Tissue-specific tritium bioaccumulation

Individual tissues were cut into finer pieces using scissors and freeze-dried, re-weighed and solubilised using 1 mL of Soluene-350 (PerkinElmer Inc., Waltham, MA, USA) at 50 °C for at least 48 h. Following solubilisation, 10 mL of liquid scintillation cocktail (Ecosint, Scientific Laboratory Supplies, UK) was added to each vial and the resulting solution was acidified with 100 μL of glacial acetic acid. Samples were then counted by liquid scintillation.

2.4. Tritium activity in the DNA

DNA was extracted from DG and gill samples using the DNeasy Blood & Tissue Kit (Qiagen) and according to the manufacturer's standard

protocol. DNA concentrations were measured using a NanoDrop® Spectrophotometer ND-1000. The quality of samples was assessed through the absorbance ratio (A260/280) and samples were considered pure when the ratio was around 1.8 (Desjardins and Conklin, 2010). Each sample was diluted to a final concentration of 25 ng μL^{-1} using Milli-Q water (Jaeschke et al., 2011). Briefly, an aliquot of the DNA solution (40 μL) was taken from each sample for scintillation counting. These were placed in clean scintillation vials with 5 mL of scintillation cocktail. Samples were kept in the dark for 90 min before scintillation counting to a fixed precision of 5 %. The mass of DNA was estimated and used to calculate the activity concentration of tritium within the DNA.

2.5. Oxidative and non-oxidative DNA damage in the haemocytes

The comet assay was performed using haemocytes of mussels (Dallas et al., 2016a,b). As a prerequisite, health status in terms of cellular viability was determined using the Trypan Blue exclusion dye assay (Strober, 2015). Samples showed >90 % viability (data not shown) and were subsequently used to determine DNA damage using the comet assay.

Oxidative damage to the DNA was performed using modified comet assay which involves adding an additional incubation step with the bacterial enzyme, formamidopyrimidine DNA glycosylase (FPG, New England Biolabs), to target oxidised purine bases (Dallas et al. 2016 a; b; Pearson et al., 2018). A single concentration of hydrogen peroxide (H_2O_2) was used as a positive control for the assay. Briefly, haemolymph samples collected from three healthy mussels were exposed under in vitro conditions to 500 μM H_2O_2 in phosphate buffer saline (1 h, in dark) and processed along with samples collected from the SW control and exposed (i.e., H-SSPs, T-SSPs, HTO) mussels. Haemolymph (150 μL) samples from six mussels were centrifuged (775 g, 2 min), the supernatant removed and the remaining cellular pellets (~10 μL) used for the assay. Cells were stained with GelRed® (10X, Cambridge Bioscience) and scored using an epifluorescent microscope (DMR; Leica Microsystems, Milton Keynes, UK). Comet IV imaging software (Perceptive Imaging, Bury St Edmunds, UK) was used to measure % tail DNA in 100 cells per slide (50 cells per microgel) (Kumaravel and Jha, 2006).

2.6. Determination of DNA methylation

Methylation levels of genomic DNA from DG and gill tissues were measured using a MethylFlash Global DNA methylation (5-mC) Quantification Kit (EpiGentek Group Inc., Farmingdale, NY, USA). A total of 100 ng of DNA was used to quantify 5-mC content following the manufacturer's protocol (EpiGentek). All samples, controls and standards were run in duplicate. The methylated fraction of DNA was detected using capture and detection antibodies and then quantified by reading the colorimetric absorbance (OD) at 450 nm using a Spectramax Plus 384 plate reader (Molecular Devices) (Teng et al., 2020; Wang et al., 2023).

To calculate percentage of methylated DNA, the standard curve was generated, and the OD values were plotted versus the positive control at each percentage point. The slope (OD/1 %) of the standard curve was determined using linear regression. The percentage of 5-methylcytosine (5-mC%) was determined using the following formula:

$$5-\mathrm{mC}\% = \frac{(\text{Sample OD} - \text{Negative control OD})}{\text{Slope} \times 2} \times 100\%$$

where the factor of 2 was used to normalise 5-mC in the positive control to 100 % (the positive control contains only 50 % of 5-mC).

2.7. Statistical analyses

2.7.1. Univariate analyses

Statistical analysis was performed using R (version 2.6.1, 2007, The R Foundation for Statistical Computing) after data were checked for normality (Shapiro-Wilk test) and equal variance (Levene's test). These assumptions were met for the water sample data, and paired Student's *t*-tests were performed to test differences between filtered and non-filtered samples. Kruskal Wallis followed by Dunn's test for multiple comparisons was performed to assess differences between time and treatments for each tissue since data did not meet the assumptions above. After confirming normality and homoscedasticity, one-way ANOVA was performed to assess tritium concentration in the DNA samples and DNA methylation differences among the treatments. When significant differences were found, the analyses were followed by Tukey's post-hoc tests. Correlations between biological responses were assessed through Spearman correlation tests. In all analyses, a p-value <0.05 was considered statistically significant.

2.7.2. Multivariate analyses

Biomarker data for mussels exposed to H-SSPs, T-SSPs and HTO were analysed using non-parametric multivariate analysis software, PRIMER v6 (PRIMER-E Ltd., Plymouth, UK; Clarke, 1999; Clarke & Warwick, 2001; Moore et al., 2021). All data were log transformed [log$n$(1+x)] and standardised to the same scale. A single value for DNA methylation in the T-SSPs treatment (7-d exposure) for the DG was clearly an extreme outlier; this value was replaced with a value obtained from the PRIMER EM (environmental) algorithm for estimating missing data values with a maximum of 1000 iterations.

Correlations between genotoxic biomarkers and tritium concentrations in DNA were tested using a scatter plot matrix (PRIMER v 6, Draftsman Plot). Principal component analysis (PCA) and hierarchical cluster analysis, derived from Euclidean distance similarity matrices, were used to visualise dissimilarities between sample groups. The results were further tested for significance using analysis of similarity (PRIMER v6 - ANOSIM), which is an approximate analogue of the univariate ANOVA and reflects on differences between treatment groups in contrast to differences among replicates within samples (the R statistic). Under the null hypothesis H_0 ("no difference between samples"), $R = 0$ and this was tested by a non-parametric permutations approach; there should be little or no effect on the average R value if the labels identifying which replicates belong to which samples are randomly rearranged.

Finally, Pearson's correlation coefficients for the biomarkers comprising the first principal component (PC1) for the integrated biomarker data from the various experimental treatments were derived. PC1 was used as an integrated measure of cellular well-being (Moore et al., 2021).

3. Results

3.1. Particles in seawater

The H-SSPs filtered stock solution showed that the most abundant particle diameter was ~140 nm. In the non-filtered stock solution, however, particle populations centred around ~250 nm and ~500 nm and a broad distribution around 1500 nm were evident (Fig. 1).

3.2. Tritium activity in seawater samples

No significant difference between filtered (0.20 μm) and non-filtered SW samples was evident with respect to tritium activities (Supplementary material 1). This suggested that tritium was released from the particles into solution or released as nanosized products after 5 h and 7 d in the presence of mussels.

3.3. Tritium bioaccumulation

Tritium concentrations in tissues of mussels collected from SW controls and H-SSPs samples were negligible or undetectable. The maximum concentrations from control and H-SSPs exposed mussels were 0.34 ×

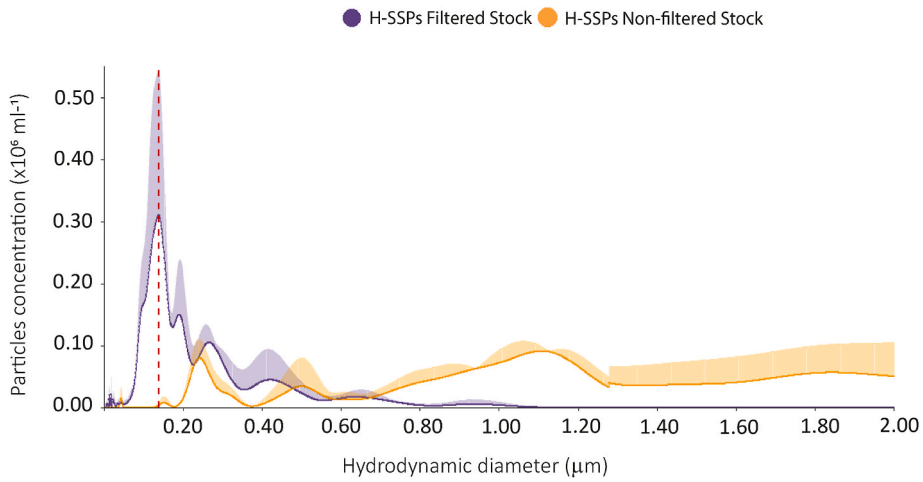

Fig. 1. The hydrodynamic diameters of hydrogenated stainless-steel particles (H-SSPs) filtered (0.22 µm) and non-filtered stock solutions in seawater (SW) measured with nanoparticle tracking analysis (Nanosight®). The shaded area corresponds to the standard deviation (SD) of measurement and the dashed line shows the most abundant particle size in the H-SSPs filtered stock solution (~140 nm).

10^{-6} MBq kg^{-1} in DG and 5.7×10^{-7} MBq kg^{-1} in other tissues, respectively. Therefore, these data were not included in Fig. 2. Some significant differences in tritium activity were found between treatments and time for each tissue (Fig. 2). No differences were observed in tissues from control mussels and those exposed to HTO for 5 h or 7 d, except in the AM of mussels exposed to 5 MBq L^{-1} after 5 h.

In DG, there was a significant increase of tritium activity after mussels were exposed to both concentrations of T-SSPs after 5 h and 7 d in comparison to the controls. The maximum concentration of tritium was found in DG after 5 h exposure to T-SSPs, showing a significant difference with mussels exposed to SW (controls) and HTO. In the AM, mussels exposed to 10 MBq L^{-1} T-SSPs for 5 h and 7 d showed an increase of tritium accumulation in comparison to controls. In the foot, mantle and 'other' tissues no significant difference was found between 5 h and 7 d exposure to 10 MBq L^{-1}, but the latter treatment resulted in a higher concentrations of tritium activity when compared to all other treatments.

3.4. Oxidative and non-oxidative DNA damage

The results indicated that oxidative DNA damage (DNA oxidation) in mussel haemocytes increased on exposure to low (1 MBq L^{-1}) and high (10 MBq L^{-1}) concentrations of T-SSPs after 5 h. Non-oxidative DNA damage was only increased after the exposure to the highest

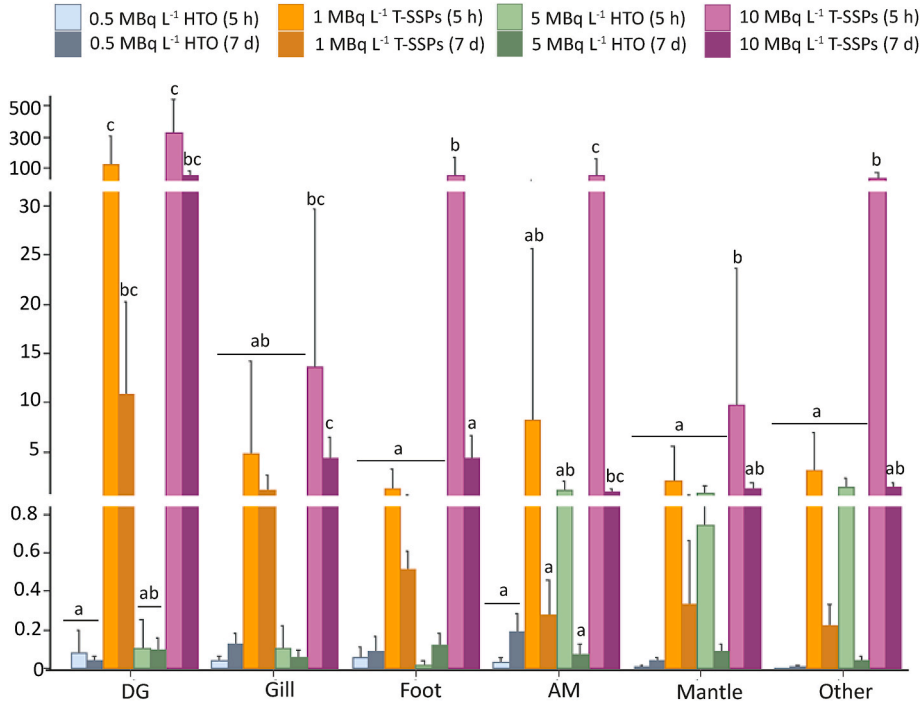

Fig. 2. Tritium activity in different tissue samples of *M. galloprovincialis* after 5 h and 7 d exposures to tritiated stainless-steel particles (T-SSPs; 1 and 10 MBq L^{-1}) and tritiated water (HTO; 0.50 and 5.0 MBq L^{-1}). Differences (Kruskal-Wallis, $p < 0.05$) between treatments for the same tissue are indicated by different lower-case letters whereas same letters show no statistical difference (e.g., after 0.50 MBq L^{-1} treatment, AM tissue showed no difference between 5 h and 7 d exposure groups ['a' and 'a' above the corresponding bars] but they were different to AM tissue exposed 5 h to 10 MBq L^{-1} ['a' and 'c' letters above the corresponding bars]. Errors bars are standard deviations for the mean of six independent determinations.

concentrations of T-SSPs and HTO after 5 h (Fig. 3 A).

After 7 d, mussels exposed to a low (1 MBq L^{-1}) and high (10 MBq L^{-1}) concentration of T-SSPs showed a significative increase of oxidative DNA damage compared to the controls (Fig. 3 B). Interestingly, mussels exposed to HTO (0.50 and 5.0 MBq L^{-1}) presented no significant oxidative DNA damage after 7 d (Fig. 3 B).

3.5. Tritium activity in the DNA

Significant differences were only found between DNA from mussel's DG exposed to T-SSPs 10 MBq L^{-1} when compared to samples from mussels exposed to H-SSPs and 0.50 MBq L^{-1} HTO (Fig. 4). The concentration of tritium in DNA was positively and significantly correlated with the tritium concentration in tissue, but no significant increase in radioactivity was observed in the DNA from gills compared to controls.

3.6. DNA methylation

In the DG after 7 d mussels exposed to H-SSPs and 0.50 HTO presented significantly higher % of DNA methylation compared to controls. However, DNA from gills obtained from mussels exposed to 1 and 5 MBq L^{-1} presented a higher percentage of DNA methylation compared to controls (Fig. 5). Interestingly, mussels exposed to H-SSPs showed a significant lower percentage of methylation compared to all other groups including the controls.

3.7. Multivariate analysis of biomarker responses

Correlation analysis (Scatter Plot matrix) of the biomarker data indicated that DNA damage and oxidative DNA damage (haemocytes) were strongly correlated after 5 h ($r = 0.560$, $p < 0.001$). PCA and hierarchical cluster analysis of the biomarkers for DNA damage and oxidative DNA damage in haemocytes following 5 h exposure showed that SSPs and HTO had a detrimental effect (Table 1; ANOSIM, $p < 0.01$) on the haemocytes of mussels (Fig. 6A), and that the first principal component (PC1) captured 54.6 % of the variation. T-SSPs and HTO treatment for 5 h induced a shift to the right (PC1) and vertically second principal component (PC2) in Euclidean Distance in the PCA that was indicative of a stress reaction (Fig. 6 A). PC1 and PC2 were both strongly correlated with DNA damage and oxidative DNA damage (PC1, $r = 0.739$ for both, $p < 0.001$; PC2, $r = 0.674$ and -0.674 respectively, $p < 0.001$).

Results showed that there were significant correlations between DNA damage and both oxidative DNA damage and DNA methylation in the gill, oxidative DNA damage and both DNA methylation in the DG (inverse) and the gill; radioactivity in the DG and both oxidative DNA damage and DNA methylation in the DG (Supplementary material 1).

ANOSIM after 7 d showed significant differences between the controls and T-SSPs 1 and T-SSPs 10 MBq L^{-1} treatment groups for DNA damage + oxidative DNA damage, controls and all experimental treatments for DNA damage + oxidative DNA damage + DNA methylation (DG and gill) (Table 1). When radioactivity (DG and gill) was included with the biomarkers, all treatments except for HTO 5 h were significantly different from the controls (Table 1). PCA and hierarchical cluster analysis of DNA damage and oxidative DNA damage showed that T-SSPs 1 and 10 MBq L^{-1} treatment groups were shifted to the right (PC1) in Euclidean Distance in the PCA that was indicative of a stress reaction (Fig. 6D).

Inclusion of DNA methylation in the MVA showed a more complex pattern with all experimental treatments being significantly different from the controls (Fig. 6C; Table 1). H-SSPs and HTO 0.5 MBq L^{-1} treatment groups were shifted vertically (PC2) and to the left (PC2), while HTO 5 and T-SSPs 1 and 10 MBq L^{-1} treatment groups were shifted horizontally to the right (PC1) and vertically (PC2) that was indicative of a stress reaction (Fig. 6 C). Further inclusion of radioactivity (DG and gill) within the combination of variables produced a similar pattern (Fig. 6 C to D), although HTO 5 h treatment was no longer significantly different from the controls (Fig. 6 D; Table 1).

Correlations between the PC1 and PC2 and the variables (biomarkers and radioactivity) following 7 d exposure are shown in Table 2. DNA damage, oxidative DNA damage and DNA methylation (DG and gill) showed very strong correlations with PC1 (Table 2).

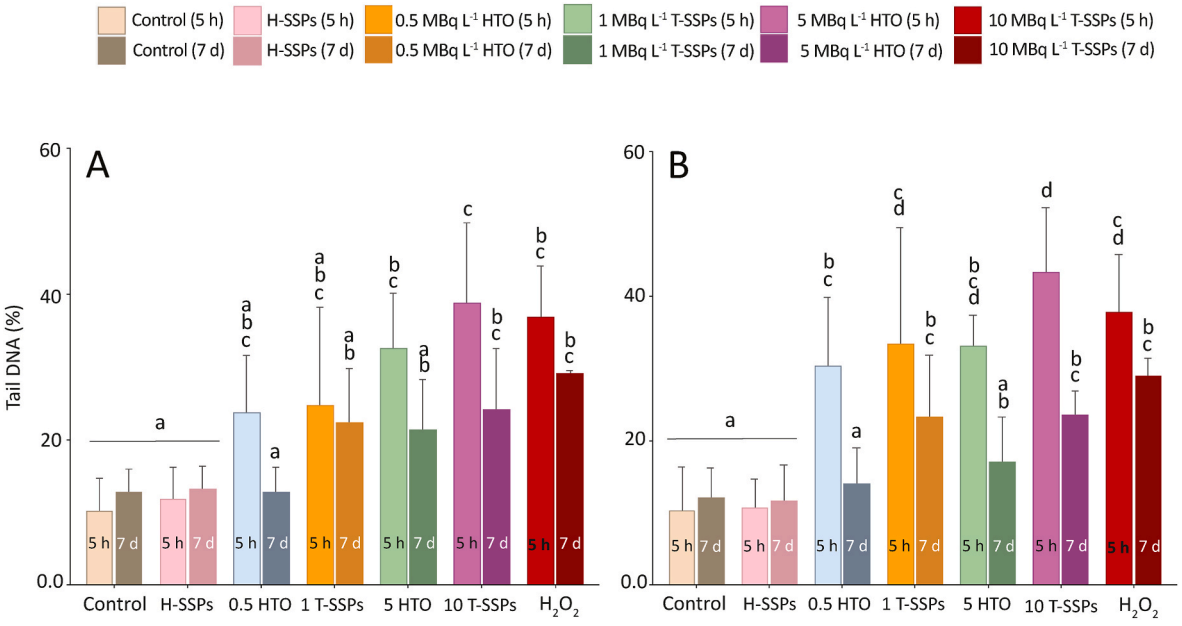

Fig. 3. Non-oxidative (A) and oxidative DNA damage (B) in *M. galloprovincialis* haemocytes after 5 h and 7 d exposures to hydrogenated (non-radioactive) stainless-steel particles (H-SSPs, 10 mg L^{-1}), tritiated stainless-steel particles (T-SSPs; 1 and 10 MBq L^{-1}), tritiated water (HTO; 0.5, 5 MBq L^{-1}) and H_2O_2 (positive control). Errors bars are standard deviations for the mean of six independent determinations. Comparisons were performed between all experimental treatments for each data set (buffer or FPG). Differences (Kruskal-Wallis, $p < 0.05$) between treatments for the same tissue are indicated by different lower-case letters whereas same letters show no statistical difference (e.g., 'a' and 'a' in controls and H-SSPs exposed groups, show no significant differences but 'a' and 'b' show significant differences among the groups, such as controls and 10 MBq L^{-1} exposed groups).

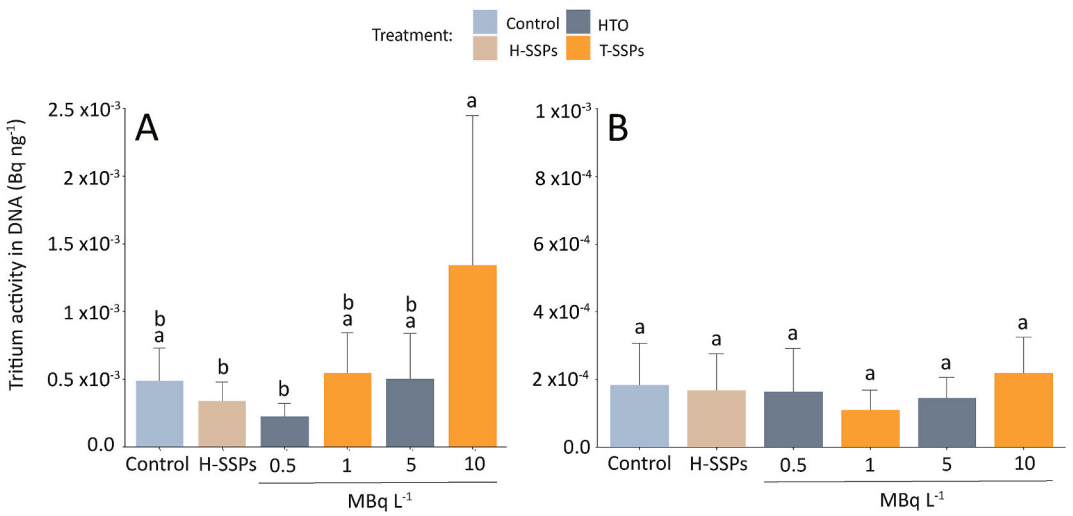

Fig. 4. Tritium activity in DNA from digestive gland (A) and gill (B) samples of mussels exposed to H-SSPs, and two different concentrations of HTO (0.5 and 5 MBq L^{-1}) and T-SSPs (1 and 10 MBq L^{-1}) for 7 d. Differences (Kruskal-Wallis, $p < 0.05$) between treatments for the same tissue are indicated by different lower case letters whereas same letters show no statistical difference (e.g., 'a' and 'a' in controls and H-SSPs exposed groups show no significant differences but 'a' and 'b' show significant differences among the groups, such as controls and 10 MBq L^{-1} exposed groups). Errors bars are standard deviations for the mean of six independent determinations.

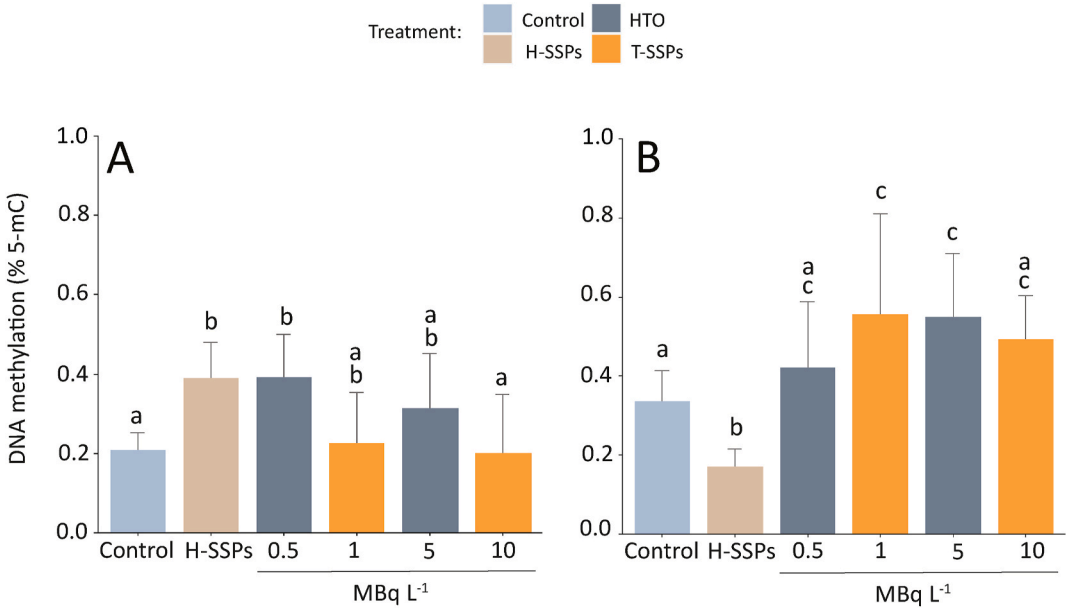

Fig. 5. DNA methylation determined as the percentage of 5-methylcytosine in digestive gland (A) and gill (B). DNA samples from mussel tissues were collected following 7 d exposure to H-SSPs and two different concentrations of HTO (0.5 and 5 MBq L^{-1}) and T-SSPs (1 and 10 MBq L^{-1}). Differences (Kruskal-Wallis, $p < 0.05$) between treatments for the same tissue are indicated by different lower-case letters whereas same letters show no statistical difference (e.g., 'b' and 'b' in H-SSPs and 0.5 MBq L^{-1} exposed groups show no significant differences but 'b' and 'c' show significant differences among the groups, such as H-SSPs and 10 MBq L^{-1} exposed groups). Errors bars are standard deviations for the mean of six independent determinations.

4. Discussion

Little is known about the behaviour, fate and toxicity of T-SSPs generated in nuclear facilities (Grisolia et al., 2019; Mentana et al., 2022; Sharpe et al., 2019). Moreover, there is limited information on toxicological and toxicokinetic studies assessing the Absorption, Distribution, Metabolism and Excretion (ADME) of stainless-steel particles in animal models (Hedberg and Odnevall Wallinder, 2016; Midander et al., 2007; Stockmann-Juvala et al., 2013). The current study provides the first elements of knowledge on T-SSPs transformation and bioaccumulation in an ecologically and economically important marine organism.

There is also a paucity of information regarding tritium concentrations in anthropogenically-impacted coastal environments (e.g., Ferreira et al., 2023). For example, following the Fukushima Daiichi nuclear power plant accident, the average tritium concentration within 1.5–30 km increased most significantly from 111.5 ± 91.1 Bq m^{-3} to approximately 513.2 ± 812.5 Bq m^{-3} but remained within the safety limits established by internationally recognized standards (Yu et al., 2025). As mentioned earlier, (section 2.2), the tritium activity concentration in the present study was selected based on projections of the dose to be received by mussels as the radiation impact is assessed in terms of dose and not on the concentrations in the environment.

Our results show that tritium can be released in nanosized particles

Table 1
Analysis of Similarity (ANOSIM) determined significance levels for the experimental treatments versus the controls after 7 d exposure for DNA damage, oxidative DNA damage, DNA methylation (DG and gill) and radioactivity (DG and gill).

ANOSIM Pairwise tests	Probability %	Probability %	Probability %	Probability %
Group	***Variables A***	***Variables B***	***Variables C***	***Variables D***
Control (SW) v H-SSPs	NS	NS	0.2	3.7
Control (SW) v 0.5 HTO	0.4	NS	0.4	1.5
Control (SW) v 1 T-SSPs	0.4	1.5	0.6	0.4
Control (SW) v 5 HTO	0.2	NS	3.2	NS
Control (SW) v 10 T-SSPs	0.2	0.4	0.2	0.2

Combinations of Variables: *A* - DNA & Oxid DNA Damage (5h); *B* - DNA & Oxid DNA Damage (7d); *C* - DNA & Oxid DNA Damage & DNA Methylation (7d); *D* - DNA & Oxid DNA Damage, DNA Methylation & Radioactivity (7d). NS – not significant.

(<0.22 μm) from the original T-SSPs, as determined by the Nanosight® and supported by scintillation counting of filtered and non-filtered seawater samples. The presence of nanosized products and/or tritium released can have been favoured for filtration and metabolic processing activities of mussels. A previous study in a freshwater mesocosm showed that a small quantity of tritium was desorbed into the freshwater column from the same batch of T-SSPs used in the present study (~16 % after 28 d; Slomberg et al., 2024). The difference observed in this study might be explained by the elevated ionic strength in the seawater coupled with tritium being weakly associated with the surface of steel particles (Slomberg et al., 2024; Sharpe et al., 2019). It might be assumed that mussels were mainly exposed to tritium as HTO and/or a nanosized particulate fraction, although it is not possible to quantify the relative importance of each form (i.e., HTO and nanosized). This is particularly so as the the concentrations, particle size distributions, hydrodynamic behaviour, uptake and tissue specific accumulation of stainless-steel particles are influenced by a range of physiochemical and biological factors.

The highest bioaccumulation of tritium was observed in the DG in line with previous studies with mussels exposed to HTO (Dallas et al., 2016a; Jha et al., 2005). In particular, tritium bioaccumulation followed a similar pattern to the accumulation of H-SSPs observed in our previous study (Vernon et al., 2022). This suggests that tritium remains at least partially associated with the particle, thereby mimicking the

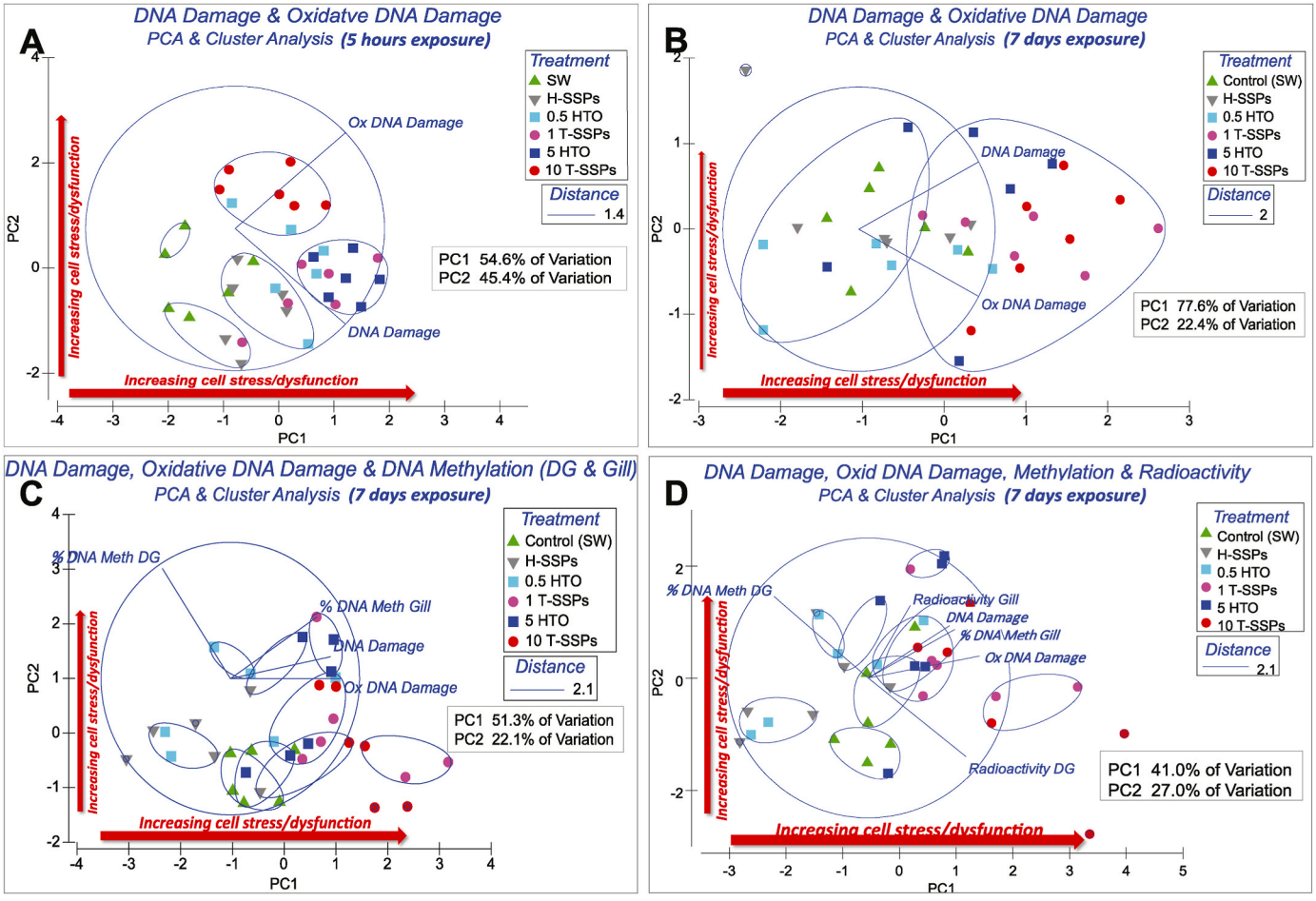

Fig. 6. Principal Component and superimposed Cluster Analysis of: A. DNA damage and oxidative DNA damage in haemocytes following 5 h exposure to H-SSPs, T-SSPs and HTO; B. DNA damage (haemocytes), oxidative DNA damage (haemocytes) following 7 d exposure; C. DNA methylation (digestive gland and gill), DNA damage (haemocytes) and oxidative DNA damage (haemocytes) following 7 d exposure; D. DNA methylation (digestive gland and gill), DNA damage (haemocytes), oxidative DNA damage (haemocytes) and radioactivity (digestive gland and gill) following 7 d exposure to H-SSPs, T-SSPs and HTO. Red arrows indicate the direction in Euclidian Space of increased cell stress and dysfunction. Blue ovals indicate the results of Cluster Analysis. (For interpretation of the references to color in this figure legend, the reader is referred to the Web version of this article.)

Table 2
Correlations for Principal Components (PC1 and PC2) and the biomarkers and radioactivity determined in two tissues following 7 d exposure.

	DNA damage	Oxid DNA damage	% DNA Meth DG	% DNA Meth Gill	Radioactivity DG	Radioactivity Gill
PC1	−0.7049***	−0.7894***	0.6660***	−0.5744***	−0.6900***	−0.2974*
PC2	0.4003**	0.1578	0.5829***	0.3736*	−0.5611***	0.5178***

*$p < 0.05$; **$p < 0.01$; ***$p < 0.001$.

bioaccumulation behaviour of its non-tritiated counterpart. Moreover, the highest concentration was observed after 5 h exposure, as evidenced in our study using chromium (Cr) as a tracer of H-SSPs (Vernon et al., 2022). This study also showed that particles are rapidly processed and egested as feces or pseudofeces within 5 h, as indicated by an increase in Cr in faeces and pseudofaeces after longer exposure periods. This further supports the observed decrease in tritium concentration in tissue and the bioaccumulation pattern across different exposure durations.

Notably, tritium bioaccumulation was higher after mussels had been exposed to the particles regardless of the concentration and time of exposure when compared to mussels exposed to HTO. Results suggest that tritium bioaccumulation is facilitated when associated with particles. Cellular uptake and digestion within the acidic endosomal/lysosomal compartments and liberation of tritium in aqueous or smaller particles might explain the enhanced bioaccumulation observed when mussels were exposed to T-SSPs. A higher retention time have been observed of nanoparticles than microparticles in mussels DG (Gonçalves et al., 2022; Wang et al., 2021b). Moreover, a small size and the relatively large surface area have been suggested to result in increased toxicity, as compared to micrometre-sized particles (Song et al., 2012; Singh et al., 2009). If the nanoparticles were to locate within the nucleus, then direct interaction between them and the DNA or DNA-related enzymes or proteins may lead to damage to the genetic material (Chen et al., 2022; Song et al., 2012). Unless particles present a lower size (<50 nm) after mussel processing, DNA damage may arise through indirect mechanisms where the nanomaterial does not physically interact with the DNA, but with other cellular proteins such as those involved in the cell division or DNA repair processes or through lipid or protein oxidation products. Additionally, they may induce oxidative stress related other cellular responses that in turn lead to genotoxicity, inflammation and aberrant signalling responses (i.e., altered transcription of genes involved in maintenance of genome integrity) (Chen et al., 2022; Moller et al., 2013; Singh et al., 2009; Song et al., 2012). Moreover, positive correlation between tritium in DG tissue and DNA indicates that tritium is internalised in the cell, providing a valuable information for further investigation in radiation dose ranges for individual cells and dose-effect relationships.

Our results also showed time and concentration dependence of genotoxic effects. After a 5 h exposure period, both concentrations of T-SSPs and a 5.0 MBq L^{-1} concentration of HTO elicited observable oxidative DNA damage in mussel haemocytes, and non-oxidative DNA damage in mussels exposed to 5 and 10 MBq L^{-1}. However, upon extending the exposure duration to 7 d, significant DNA damage was not observed in most treatments, except for mussels exposed to the lower concentration of T-SSPs. These results align with a prior report of genetic damage in human lung cells following in vitro exposure to different concentrations of T-SSPs (5–100 MBq L^{-1}) after 2 and 24 h exposures (Lamartiniere et al., 2022). The authors highlighted that while T-SSPs may induce DNA double-strand breaks (DSBs) in affected cells, most cells in the population may remain "unexposed," resulting in a low expected yield of radiation-induced DSBs. Moreover, the onset of repair mechanisms may contribute to the observed lack of DNA damage after 7 d in most treatments or loss of heavily damaged cells. Praveen Kumar et al. (2014) assessed DNA damage in haemocytes of clams using the comet assay at various time points (24, 48 and 72 h) post-irradiation with different doses of gamma radiation (2–10 Gy). The highest DNA damage was observed at 24 h post-treatment, followed by a considerable decrease in damage over time and reaching a minimum at 72 h post-treatment for all doses. This decrease in genetic damage at later times may indicate either repair of damaged DNA or loss of heavily damaged cells, or both, as suggested by Banu et al. (2001) and Revankar and Shyama (2009). Further exploration of these repair mechanisms and their temporal cellular dynamics is crucial for comprehensive understanding of the genotoxic response of the organisms to T-SSPs and HTO.

DNA methylation patterns showed an increase in gill tissues after mussels were exposed to 1 and 5 MBq L^{-1} of T-SSPs and HTO, respectively. Conversely, mussels exposed to H-SSPs exhibited decreased DNA methylation compared to the controls, suggesting differential effects of pollutants on epigenetic regulation. This response was positively correlated with oxidative and non-oxidative DNA damage. In the DG, however, no difference was observed between treatments and the response was negatively correlated with oxidative DNA damage and the tritium concentration in DNA. This can be explained by the induction of demethylation process through the presence of ROS (Belli and Tabocchini, 2020; Kong et al., 2016), and suggests that DNA methylation response is concentration and tissue-specific as previously reported in bivalves and mice (Akcha et al., 2021; Koturbash et al., 2006; Pogribny et al., 2004; Siegfried and Simon, 2010; Tawa et al., 1998).

Toxicity or cellular injury induced by any environmental agent is a tissue-specific phenomenon. This is attributed to metabolic capacity of the tissues, which also include differential generation of ROS and DNA repair capabilities (Jha, 2008). The variability in tissue specific DNA methylation pattern could also result from these inherent differential properties of the of the tissues. Previous studies have shown that DNA methylation can regulate the expression of gene families involved in stress and environmental responses (Gavery and Roberts, 2010). Akcha et al. (2021) observed that oysters exposed to diuron herbicide (0.20–0.30 μg L^{-1} for 7d) presented a decrease in global DNA methylation of oyster tissues. However, hypermethylation was detected in the digestive gland, whereas diuron exposure had no effect on gill and gonadal tissues. The study reinforces the premise that these epigenetic changes are tissue specific as observed in the present study.

Tritium concentration in the DG was positively correlated with the oxidative DNA damage in haemocytes. This is expected considering the generation of ROS by radiation, the enhanced tritium bioaccumulation in DG and the fact that haemocytes as circulating cells are exposed to tritium during the water filtration process.

The use of PCA as an indicator of cell health status space was clearly demonstrated in the present study, where a very strong inverse correlation of PC1 for DNA damage and oxidative DNA damage was indicated after 5 h and 7 d exposures. Moreover, the combination of DNA damage, oxidative DNA damage and DNA methylation was the most effective set of biomarkers (variables) for elucidating the adverse effects of the H-SSPs, T-SSPs and HTO treatments. The application of MVA to the biomarker data has shown that the various experimental treatments differed from the controls. Furthermore, this investigation has indicated that PCA can be used effectively as an integrated indicator of cell health status when using appropriate combinations of molecular and cell biomarkers such as DNA damage and oxidative DNA damage (Sforzini et al., 2018, 2020; Moore et al., 2021).

5. Conclusions

Our work represents the first study of T-SSPs, an environmentally relevant contaminant, in a representative marine organism. It also presents the first report of epigenetic effects of a globally significant

radioactive particles in marine bivalves. Our results showed the importance of considering tritium form (HTO versus tritium associated with particles) to determine its behaviour in SW as well as tritium bioaccumulation and genotoxic effects. Moreover, assessing tissue-specific bioaccumulation is essential for understanding potential epigenetic effects that have been shown to vary among the tissues with wider biological significance in relation to radiation exposures. Epigenetic effects, which link genotype and phenotype by influencing gene expression, can be passed through generations (Horemans et al., 2019; Kamstra et al., 2018; Trijau et al., 2018). These heritable DNA methylation patterns may regulate stress responses and facilitate adaptation to local stressors with significant implications for environmental risk assessment. Further investigation is needed to disentangle the relationship and mechanisms of epigenetic effects induced by radiation to understand the impact of radionuclides at higher levels of biological organisation.

CRediT authorship contribution statement

Maria Florencia Ferreira: Writing – review & editing, Writing – original draft, Methodology, Investigation, Formal analysis, Data curation, Conceptualization. **Andrew Turner:** Writing – review & editing, Methodology, Conceptualization. **Mickaël Payet:** Methodology, Investigation. **Olivier Debellemaniere:** Methodology, Investigation. **Christian Grisolia:** Project administration. **Veronique Malard:** Writing – review & editing. **Michael N. Moore:** Writing – review & editing, Formal analysis. **Awadhesh N. Jha:** Writing – review & editing, Writing – original draft, Supervision, Resources, Project administration, Investigation, Funding acquisition, Conceptualization.

Declaration of competing interest

The authors declare that they have no known competing financial interests or personal relationships that could have appeared to influence the work reported in this paper.

Acknowledgements

The work has been carried out within the TRANSAT and TITANS projects which received funding from the Euratom research and innovation programme 2014–2018 (grant agreement No. 754586) and 2022–2025 (grant agreement No. 101059408), respectively. The authors thank the Molecular Labelling and Bio-organic Chemistry (SCBM) unit at CEA Paris-Saclay. The opinions expressed herein reflect only the authors' views and do not necessarily reflect those of the European Commission.

Appendix A. Supplementary data

Supplementary data to this article can be found online at https://doi.org/10.1016/j.envpol.2025.127002.

Data availability

Data will be made available on request.

References

Adam-guillermin, C., Pereira, S., Della-vedova, C., 2012. Genotoxic and reprotoxic effects of tritium and external gamma irradiation on aquatic animals. Rev. Environ. Contam. Toxicol. 220. https://doi.org/10.1007/978-1-4614-3414-6.

Akcha, F., Barranger, A., Bachère, E., 2021. Genotoxic and epigenetic effects of diuron in the Pacific oyster: in vitro evidence of interaction between DNA damage and DNA methylation. Environ. Sci. Pollut. Control Ser. 28 (7), 8266–8280. https://doi.org/10.1007/s11356-020-11021-6.

Banu, S., Danadevi, K., Jamil, K., Ahuja, R., Visweswara Rao, K., Ishaq, M., 2001. In vivo genotoxic effect of arsenic trioxide in mice using comet assay. Toxicology 162 (3), 171–177.

Barreira, J., Araújo, D.F., Knoery, J., Briant, N., Machado, W., Grouhel-Pellouin, A., 2024. The French mussel watch program reveals the attenuation of coastal lead contamination over four decades. Mar. Pollut. Bull. 199, 115975 h ttps://doi.org/10.1016/j.marpolbul.2023.115.

Belli, M., Tabocchini, M.A., 2020. Ionizing radiation-induced epigenetic modifications and their relevance to radiation protection. Int. J. Mol. Sci. 21 (17), 5993. https://doi.org/10.3390/ijms21175993.

Chen, Z., Shi, J., Zhang, Y., Han, S., Zhang, J., Jia, G., 2022. DNA oxidative damage as a sensitive genetic endpoint to detect the genotoxicity induced by titanium dioxide nanoparticles. Nanomaterials 12 (15), 2616. https://doi.org/10.3390/nano12152616.

Clarke, R., 1999. Non-metric multivariate analysis in community-level ecotoxicology. Environ. Toxicol. Chem. 18 (2), 117–127.

Clarke, K.R., Warwick, R.M., 2001. Change in Marine Communities: an Approach to Statistical Analysis and Interpretation. PRIMER-e, Plymouth, UK.

Dallas, L.J., Bean, T.P., Turner, A., Lyons, B.P., Jha, A.N., 2013. Oxidative DNA damage may not mediate Ni-induced genotoxicity in marine mussels: assessment of genotoxic biomarkers and transcriptional responses of key stress genes. Mutat. Res. Genet. Toxicol. Environ. Mutagen 754, 22–31. https://doi.org/10.1016/j.mrgentox.2013.03.009.

Dallas, L.J., Bean, T.P., Turner, A., Lyons, B.P., Jha, A.N., 2016a. Exposure to tritiated water at an elevated temperature: Genotoxic and transcriptomic effects in marine mussels (*M. galloprovincialis*). J. Environ. Radioact. 164, 325–336. https://doi.org/10.1016/j.jenvrad.2016.07.034.

Dallas, L.J., Devos, A., Fievet, B., Turner, A., Lyons, B.P., Jha, A.N., 2016b. Radiation dose estimation for marine mussels following exposure to tritium: best practice for use of the ERICA tool in ecotoxicological studies. J. Environ. Radioact. 155–156, 1–6. https://doi.org/10.1016/j.jenvrad.2016.01.019.

Desjardins, P., Conklin, D., 2010. NanoDrop microvolume quantitation of nucleic acids. JoVE J. 22 (45), 2565. https://doi.org/10.3791/2565.

Eyrolle, F., Ducros, L., Le Dizès, S., Beaugelin-Seiller, K., Charmasson, S., Boyer, P., Cossonnet, C., 2018. An updated review on tritium in the environment. J. Environ. Radioact. 181, 128–137. https://doi.org/10.1016/j.jenvrad.2017.11.001.

Ferreira, M.F., Turner, A., Payet, M., Grisolia, C., Lebaron-Jacobs, L., Malard, V., Jha, A. N., 2023. Tritium: its relevance, sources and impacts on non-human biota. Sci. Total Environ., 162816 https://doi.org/10.1016/j.scitotenv.2023.162816.

Ferreira, M.F., Turner, A., Vernon, E.L., Grisolia, C., Malard, V., Moore, M., Jha, A.N., 2024. Bioaccumulation and biological effects of hydrogenated cement particles in the marine bivalve, *Mytilus galloprovincialis*. Chemosphere 359, 142243. https://doi.org/10.1016/j.chemosphere.2024.142243.

Gavery, M.R., Roberts, S.B., 2010. DNA methylation patterns provide insight into epigenetic regulation in the Pacific oyster (*Crassostrea gigas*). BMC Genom. 11, 483. https://doi.org/10.1186/1471-2164-11-483.

Gonçalves, J.M., Sousa, V.S., Teixeira, M.R., Bebianno, M.J., 2022. Chronic toxicity of polystyrene nanoparticles in the marine mussel *Mytilus galloprovincialis*. Chemosphere 287, 132356. https://doi.org/10.1016/j.chemosphere.2021.132356.

Grisolia, C., Gensdarmes, F., Peillon, S., Dougniaux, G., Bernard, E., Autricque, A., Pieters, G., Rousseau, B., Feuillastre, S., Garcia-Argote, S., Carvalho, O., Malard, V., George, I., Lebaron-Jacobs, L., Orsiere, T., Uboldi, C., Rose, J., Sanles Sobrido, M., Lambertin, D., Vrel, D., Decanis, C., Liger, K., Acsente, T., Dinescu, G., 2019. Current investigations on tritiated dust and its impact on tokamak safety. Nucl. Fusion 59, 086061. https://doi.org/10.1088/1741-4326/ab1a76.

Hanslík, E., Marešová, D., Juranová, E., Sedlářová, B., 2017. Comparison of balance of tritium activity in waste water from nuclear power plants and at selected monitoring sites in the Vltava River, Elbe River and Jihlava (Dyje) River catchments in the Czech Republic. J. Environ. Manag. 203, 1137–1142. https://doi.org/10.1016/j.jenvman.2017.06.056.

Hedberg, Y.S., Odnevall Wallinder, I., 2016. Metal release from stainless steel in biological environments: a review. Biointerphases 11, 018901. https://doi.org/10.1116/1.4934628.

Horemans, N., Spurgeon, D.J., Lecomte-Pradines, C., Saenen, E., Bradshaw, C., Oughton, D., Rasnaca, I., Kamstra, J.H., Adam-Guillermin, C., 2019. Current evidence for a role of epigenetic mechanisms in response to ionizing radiation in an ecotoxicological context. Environ. Pollut. 251, 469–483. https://doi.org/10.1016/j.envpol.2019.04.125.

Jaenisch, R., Bird, A., 2003. Epigenetic regulation of gene expression: how the genome integrates intrinsic and environmental signals. Nat. Genet. 33, 245–254. https://doi.org/10.1038/ng1089.

Jaeschke, B.C., Bradshaw, C., 2013. Bioaccumulation of tritiated water in phytoplankton and trophic transfer of organically bound tritium to the blue mussel, Mytilus edulis. J. Environ. Radioact. 115, 28–33. https://doi.org/10.1016/j.jenvrad.2012.07.008.

Jaeschke, B.C., Millward, G.E., Moody, A.J., Jha, A.N., 2011. Tissue-specific incorporation and genotoxicity of different forms of tritium in the marine mussel, *Mytilus edulis*. Environ. Pollut. 159, 274–280. https://doi.org/10.1016/J.ENVPOL.2010.08.033.

Jha, A.N., 2008. Ecotoxicological applications and significance of the comet assay. Mutagenesis 23, 207–221. https://doi.org/10.1093/MUTAGE/GEN014.

Jha, A.N., Dogra, Y., Turner, A., Millward, G.E., 2005. Impact of low doses of tritium on the marine mussel, *Mytilus edulis*: genotoxic effects and tissue-specific bioconcentration. Mutat. Res. Genet. Toxicol. Environ. Mutagen 586, 47–57. https://doi.org/10.1016/j.mrgentox.2005.05.008.

Jha, A., Ferreira, M.F., Vernon, E., Turner, A., 2022. Report on ecotoxicological and genotoxicological impact on tritiated and untritiated particles on marine bivalves. https://transat-h2020.eu.

Jong, M.C., Li, J., Noor, H.M., He, Y., Gin, K.Y.H., 2022. Impacts of size-fractionation on toxicity of marine microplastics: enhanced integrated biomarker assessment in the

tropical mussels, *Perna viridis*. Sci. Total Environ. 835, 155459. https://doi.org/10.1016/j.scitotenv.2022.155459.
Kaizer, J., Hirose, K., Povinec, P.P., 2024. Assessment of environmental impacts from authorized discharges of tritiated water from the Fukushima site to coastal and offshore regions. J. Environ. Radioact. 278, 107507. https://doi.org/10.1016/j.jenvrad.2024.107507.
Kamstra, J.H., Hurem, S., Martin, L.M., Lindeman, L.C., Legler, J., Oughton, D., Salbu, B., Anders, D., Lyche, j., Aleström, P., 2018. Ionizing radiation induces transgenerational effects of DNA methylation in zebrafish. Sci. Rep. 8 (1), 15373.
Kong, E.Y., Cheng, S.H., Yu, K.N., 2016. Zebrafish as an in vivo model to assess epigenetic effects of ionizing radiation. Int. J. Mol. Sci. 17 (12), 2108. https://doi.org/10.3390/ijms17122108.
Koturbash, I., Rugo, R.E., Hendricks, C.A., Loree, J., Thibault, B., Kutanzi, K., Pogribny, I., Yanch, J.C., Engelward, B.P., Kovalchuk, O., 2006. Irradiation induces DNA damage and modulates epigenetic effectors in distant bystander tissue in vivo. Oncogene 25, 4267–4275. https://doi.org/10.1038/sj.onc.1209467.
Kovalchuk, O., Baulch, J.E., 2008. Epigenetic changes and nontargeted radiation effects - is there a link? Environ. Mol. Mutagen. 49 (1), 16–25. https://doi.org/10.1002/em.20361.
Kovalchuk, O., Burke, P., Besplug, J., Slovack, M., Filkowski, J., Pogribny, I., 2004. Methylation changes in muscle and liver tissues of male and female mice exposed to acute and chronic low-dose X-ray-irradiation. Mutat. Res. Fundam. Mol. Mech. Mutagen. 548, 75–84. https://doi.org/10.1016/j.mrfmmm.2003.12.016.
Kumar, S., Singh, A.K., Mohapatra, T., 2017. Epigenetics: history, present status and future perspective. Indian J. Genet. Plant Breed. 77 (4), 445–463. https://doi.org/10.5958/0975-6906.2017.00061.X.
Kumaravel, T.S., Jha, A.N., 2006. Reliable Comet assay measurements for detecting DNA damage induced by ionising radiation and chemicals. Mutat. Res., Genet. Toxicol. Environ. Mutagen. 605, 7–16. https://doi.org/10.1016/J.MRGENTOX.2006.03.002.
Lamartiniere, Y., Slomberg, D., Payet, M., Tassistro, V., Mentana, A., Baiocco, G., Rose, J., Lebaron-Jacobs, L., Grisolia, C., Malard, V., Orsière, T., 2022. Cyto-Genotoxicity of tritiated stainless steel and cement particles in human lung cell models. Int. J. Mol. Sci. 23 (18), 10398. https://doi.org/10.3390/ijms231810398.
Liger, K., Grisolia, C., Cristescu, I., Moreno, C., Malard, V., Coombs, D., Markelj, S., 2018. Overview of the TRANSAT (TRANSversal actions for tritium) project. Fusion Eng. Des. 136, 168–172. https://doi.org/10.1016/j.fusengdes.2018.01.037.
Mentana, A., Lamartinière, Y., Orsière, T., Malard, V., Payet, M., Slomberg, D., Guardamagna, I., Lonati, L., Grisolia, C., Jha, A., Lebaron-Jacobs, L., Rose, J., Ottolenghi, A., Baiocco, G., 2022. Tritiated steel micro-particles: computational dosimetry and prediction of radiation-induced DNA damage for in vitro cell culture exposures. Radiat. Res. 199, 25–38. https://doi.org/10.1667/RADE-22-00043.1.
Midander, K., Pan, J., Odnevall Wallinder, I., Leygraf, C., 2007. Metal release from stainless steel particles in vitro - influence of particle size. J. Environ. Monit. 9, 74–81. https://doi.org/10.1039/b613919a.
Moller, P., Danielsen, P.H., Jantzen, K., Roursgaard, M., Loft, S., 2013. Oxidatively damaged DNA in animals exposed to particles. Crit. Rev. Toxicol. 43, 96–118. https://doi.org/10.3109/10408444.2012.756456.
Moore, M.N., Sforzini, S., Viarengo, A., Barranger, A., Aminot, Y., Readman, J.W., Khlobystov, A.N., Arlt, V.M., Banni, M., Jha, A.N., 2021. Antagonistic cytoprotective effects of C60 fullerene nanoparticles in simultaneous exposure to benzo[a]pyrene in a molluscan animal model. Sci. Total Environ. 755, 142355. https://doi.org/10.1016/j.scitotenv.2020.142355.
Nie, B., Fang, S., Jiang, M., Wang, L., Ni, M., Zheng, J., Yang, Z., Li, F., 2021. Anthropogenic tritium: inventory, discharge, environmental behaviour and health effects. Renew. Sustain. Energy Rev. 135, 110188. https://doi.org/10.1016/j.rser.2020.110188.
Oms, E., Bailly du Bois, P., Dumas, F., Lazure, P., Morillon, M., Voiseux, C., Corre, C.L., Cossonnet, C., Solier, L., Morin, P., 2019. Inventory and distribution of tritium in the oceans in 2016. Sci. Total Environ. 656, 1289–1303. https://doi.org/10.1016/j.scitotenv.2018.11.448.
Pearson, H., Dallas, L.J., Comber, S.D.W., Braungardt, C.B., Worsfold, P.J., Jha, A.N., 2018. Mixtures of tritiated water, zinc and dissolved organic carbon: assessing interactive bioaccumulation and genotoxic effects in marine mussels, *Mytilus galloprovincialis*. J. Environ. Radioact. 187, 133–143. https://doi.org/10.1016/j.jenvrad.2017.12.018.
Pogribny, I., Raiche, J., Slovack, M., Kovalchuk, O., 2004. Dose-dependence, sex- and tissue-specificity, and persistence of radiation-induced genomic DNA methylation changes. Biochem. Biophys. Res. Commun. 320, 1253–1261. https://doi.org/10.1016/j.bbrc.2004.06.081.
Praveen Kumar, M.K., Shyama, S.K., Sonaye, B.S., Roshini Naik, S., Kadam, S.B., Bipin, P. D., D'costa, A., Chaubey, R.C., 2014. Evaluation of γ-radiation-induced DNA damage in two species of bivalves and their relative sensitivity using comet assay. Aquat. Toxicol. 150, 1–8. https://doi.org/10.1016/j.aquatox.2014.02.007.
Reisz, J.A., Bansal, N., Qian, J., Zhao, W., Furdui, C.M., 2014. Effects of ionizing radiation on biological molecules - mechanisms of damage and emerging methods of detection. Antioxidants Redox Signal. 21 (2), 260–292. https://doi.org/10.1089/ars.2013.5489.
Revankar, R.R., Shyama, S.K., 2009. Genotoxic effects of monocrotophos, an organophosphorous pesticide, on an estuarine bivalve, *Meretrix ovum*. Food Chem. Toxicol. 47 (7), 1618–1623.
Sforzini, S., Moore, M.N., Oliveri, C., Volta, A., Jha, A., Banni, M., Viarengo, A., 2018. Role of mTOR in autophagic and lysosomal reactions to environmental stressors in molluscs. Aquat. Toxicol. 195, 114–128. https://doi.org/10.1016/j.aquatox.2017.12.014.
Sforzini, S., Oliveri, C., Barranger, A., Jha, A.N., Banni, M., Moore, M.N., Viarengo, A., 2020. Effects of fullerene C60 in blue mussels: role of mTOR in autophagy related cellular/tissue alterations. Chemosphere 246, 125707. https://doi.org/10.1016/J.CHEMOSPHERE.2019.125707.
Sharpe, M., Fagan, C., Shmayda, W.T., 2019. Distribution of tritium in the near surface of type 316 stainless steel. Fusion Sci. Technol. 75, 1053–1057. https://doi.org/10.1080/15361055.2019.1644136.
Siegfried, Z., Simon, I., 2010. DNA methylation and gene expression. WIREs Systems Biology and Medicine 2, 362–371. https://doi.org/10.1002/wsbm.64.
Singh, N., Manshian, B., Jenkins, G.J.S., Griffiths, S.M., Williams, P.M., Maffeis, T.G.G., Wright, C.J., Doak, S.H., 2009. NanoGenotoxicology: the DNA damaging potential of engineered nanomaterials. Biomaterials 30, 23–24. https://doi.org/10.1016/j.biomaterials.2009.04.009.
Slomberg, D.L., Auffan, M., Payet, M., Carboni, A., Ouaksel, A., Brousset, L., Angeletti, B., Grisolia, C., Thiéry, A., Rose, J., 2024. Tritiated stainless steel (nano)particle release following a nuclear dismantling incident scenario: significant exposure of freshwater ecosystem benthic zone. J. Hazard Mater. 465, 133093. https://doi.org/10.1016/j.jhazmat.2023.133093.
Song, M.F., Li, Y.S., Kasai, H., Kawai, K., 2012. Metal nanoparticle-induced micronuclei and oxidative DNA damage in mice. J. Clin. Biochem. Nutr. 50, 211–216. https://doi.org/10.3164/jcbn.11-70.
Stockmann-Juvala, H., Hedberg, Y., Dhinsa, N.K., Griffiths, D.R., Brooks, P.N., Zitting, A., Wallinder, I.O., Santonen, T., 2013. Inhalation toxicity of 316L stainless steel powder in relation to bioaccessibility. Hum. Exp. Toxicol. 32, 1137–1154. https://doi.org/10.1177/0960327112472354.
Strober, W., 2015. Trypan blue exclusion test of cell viability. Curr. Protoc. Im. 111. https://doi.org/10.1002/0471142735.IMA03BS111. A3.B.1.
Tawa, R., Yutaka, K., Jum-Ichiro, K., Miyamura, Y., Kurishita, A., Sasaki, M., Sakurai, H., Ono, T., 1998. Effects on X-ray irradiation on genomic DNA mehtylation levels in mouse tissue. J. Radiat. Res. 39, 271–278.
Teng, M., Chen, X., Wang, Chen, Song, M., Zhang, J., Bi, S., Wang, Chengju, 2020. Life cycle exposure to propiconazole reduces fecundity by disrupting the steroidogenic pathway and altering DNA methylation in zebrafish (*Danio rerio*). Environ. Int. 135, 105384. https://doi.org/10.1016/j.envint.2019.105384.
Trijau, M., Asselman, J., Armant, O., Adam-Guillermin, C., De Schamphelaere, K.A.C., Alonzo, F., 2018. Transgenerational DNA methylation changes in Daphnia magna exposed to chronic γ irradiation. Environ. Sci. Technol. 52, 4331–4339. https://doi.org/10.1021/acs.est.7b05695.
Varlam, C., Stefanescu, I., Patrascu, V., Varlam, M., Raceanu, M., Enache, A., Bucur, C., 2005. The use of tritiated wastewater from NPP cernavoda to estimate maximum soluble pollutants on Danube - Black Sea Channel. In: Fusion Science and Technology. American Nuclear Society, pp. 716–719. https://doi.org/10.13182/FST05-A1024.
Vernon, E.L., Jha, A.N., Ferreira, M.F., Slomberg, D.L., Malard, V., Grisolia, C., Payet, M., Turner, A., 2022. Bioaccumulation, release and genotoxicity of stainless-steel particles in marine bivalve molluscs. Chemosphere 303, 134914. https://doi.org/10.1016/J.CHEMOSPHERE.2022.134914.
Wang, Y., Jorda, M., Jones, P.L., Maleszka, R., Ling, X., Robertson, H.M., Craig, M., Peinado, M.A., Robinson, G.E., 2006. Functional CpG methylation system in a social insect. Science 314, 645–647. https://doi.org/10.1126/science.1135213, 1979.
Wang, S., Hu, M., Zheng, J., Huang, W., Shang, Y., Kar-Hei Fang, J., Shi, H., Wang, Y., 2021a. Ingestion of nano/micro plastic particles by the mussel *Mytilus coruscus* is size dependent. Chemosphere 263, 127957. https://doi.org/10.1016/j.chemosphere.2020.127957.
Wang, S., Zhong, Z., Li, Z., Wang, X., Gu, H., Huang, W., Fang, J.K.H., Shi, H., Hu, M., Wang, Y., 2021b. Physiological effects of plastic particles on mussels are mediated by food presence. J. Hazard Mater. 404, 124136. https://doi.org/10.1016/j.jhazmat.2020.124136.
Wang, X., Cong, R., Li, A., Wang, W., Zhang, G., Li, L., 2023. Experimental DNA demethylation reduces expression plasticity and thermal tolerance in Pacific oysters. Mar. Biotechnol. 25, 341–346. https://doi.org/10.1007/s10126-023-10208-5.
Ward, J.E., Zhao, S., Holohan, B.A., Mladinich, K.M., Griffin, T.W., Wozniak, J., Shumway, S.E., 2019. Selective ingestion and egestion of plastic particles by the blue mussel (*Mytilus edulis*) and eastern oyster (*Crassostrea virginica*): implications for using bivalves as bioindicators of microplastic pollution. Environ. Sci. Technol. 53, 8776–8784. https://doi.org/10.1021/acs.est.9b02073.
Wei, J., Wang, B., Wang, H., Meng, L., Zhao, Q., Li, X., Xin, Y., Jiang, X., 2019. Radiation-induced normal tissue damage: oxidative stress and epigenetic mechanisms. Oxid. Med. Cell. Longev. 11. https://doi.org/10.1155/2019/3010342.
Yu, Z., Shen, Z., Shi, Z., Fang, W., Liu, X., Yu, W., Cai, M., 2025. The spatial and temporal variations in tritium in the North Pacific over the past 70 years and their impacts on the marine environment and organisms. J. Geophys. Res.: Oceans 130, e2024JC022058. https://doi.org/10.1029/2024JC022058.